Original Paper

Landslides
DOI 10.1007/s10346-010-0244-6
Received: 11 June 2010
Accepted: 1 November 2010

Thomas Lebourg · Hernandez Mickael · Jomard Hervé · El Bedoui Samyr · Bois Thomas · Zerathe Swann · Tric Emmanuel · Vidal Maurin

Temporal evolution of weathered cataclastic material in gravitational faults of the La Clapiere deep-seated landslide by mechanical approach

Abstract After a few years of research, the observation and the analysis of the deep-seated landslides suggest that these are mainly controlled by tectonic structures, which play a dominant role in the deformation of massif slopes. The La Clapière deep-seated landslide (Argentera Mercantour massif) is embedded in a deep-seated gravitational slope deformation affecting the entire slope, and characterized by specific landforms (trenches, scarps…). Onsite, the tangential displacement direction of the trenches and the scarps are controlled by the tectonic structures. The reactivation of the inherited fault in gravitational faults create a gouge material exposed to an additional mechanical and chemical weathering as well as an increased of leaching. The displacement of these reactivated faults gets increasingly important around the area of the La Clapière landslide and this since 3.6ka BP. In this study, mechanical analysis and grain size distributions were performed and these data were analysed according to their proximity the La Clapiere landslide and times of initiation of the landslide by ^{10}Be dating. Triaxial test results show that the effective cohesion decreases and the effective angle of internal friction increases from the unweathered area to the weathered area. The whole distribution of the grain size indicates that the further the shear zone is open or developed, the further the residual material loses its finest particles. This paper suggests that the mechanical evolution along the reactivated fault is influenced by the leaching processes. For the first time, we can extract from these data temporal behaviour of the two main mechanical parameters (cohesion and angle of internal friction) from the beginning of the La Clapiere landslide initiation (3.6 ka BP) to now.

Keywords Weathering · Gravitational fault · La Clapière landslide · Temporal evolution

Introduction

Phenomena involved in landslides are complex and depend on numerous parameters such as their structure, composition, history and climate conditions. Among these, the regional geological history plays a key role (Agliardi et al. 2001).

On the Argentera Mercantour massif scale, inherited faults are accurately mapped (Follaci et al. 1988; Guglielmi et al. 2002). Guglielmi et al. (2005) suggest that the La Clapière deep-seated landslide is controlled by tectonic structures. Cappa et al. (2004) and Jomard (2006) show that the La Clapière landslide is imbedded in a deep-seated gravitational slope deformation (DSGSD). It affects the overall slope and is characterized by specific landforms (double-crested ridges, trenches, scarps, ridge depressions and sliding surfaces).

During the evolution of DSGSD zones, the strain accommodation should have been led by the weakest zones of the massif, in particular by the inherited tectonic framework. This strain accommodation is characterized by the reactivation of inherited faults which are expressed in the morphology by the original specific landforms (Jomard 2006).

The reactivated faults are characterized by weathered cataclastic gneissic material, coming from weathering processes (macro and micro mechanical destructuration and hydrolysis weathering). These processes are very important predisposed factors for slope instabilities. Pronounced weathering conditions determine meaningful reductions in shear strength of the bed rock and a consequent increase in possible slope failures (Cascini et al. 1992; Jaboyedoff et al. 2004). The efficiency of the weathering processes depend mainly on the fractured state of rock mass (Gerber and Scheidegger 1969; Durville and Lacube 1992) and also on climate conditions and the physical rock characteristics (Selby 1993).

Once the gravitational movement has been initiated, the reactivation increases the displacement rate within the shear zone. It influences the quantity of the crushing applied on cataclastic material. The consequence of the localization of the deformation on faults will decrease the mechanical shearing resistance. The consecutive modification in the shape and the particle size distribution of this material influences the evolution of the mechanical behaviour in these failure zones (Lebourg et al. 2003, 2004; Jaboyedoff et al. 2004).

This study focuses on cataclastic gneissic material rheology within reactived faults. Jomard et al. (2006) observed an effective cohesion (c') decrease and an effective angle of internal friction (φ') increase from the unweathered area to the weathered area by studying the cataclastic gneissic material sampled in one gravitational fault. These results express the mechanical state of this weathered cataclastic gneissic material. Other reactivated faults have a similar distribution as far as mechanical parameters are concerned. The principal aim of this study is to extend the previous investigation and laboratory tests field (Jomard et al. 2006) to other discontinuities in order to: (1) suggest another interpretation based on the whole results obtained and (2) extract for the first time temporal behaviours of mechanical parameter for gneissic material in the goal to constrain in the future numerical approaches.

In this study, we choose to work on three non-gravitational faults and three gravitational faults segments recognise by Jomard (2006), dated by ^{10}Be (Bigot-Cormier et al. 2005) and analysed as a model of progressive failure by El Bedoui (El Bedoui et al. 2009). El Bedoui show three phases of the deformation of the landslide guided by these gravitational faults, and this at three different time scale: a first step with an initial slow slope deformation, spreading from the foot to the top, from 10–5.6 ka BP; a second step with an increase in the average displacement

Published online: 08 January 2011

from the foot to the middle of the slope, from 5.6 to 3.6 ka BP and a third step with the development of a large failure at the foot of the slope with fast displacement from 3.6 ka BP to now with the opening of the gravitational faults.

In this paper, we first present the study area, the morphology of inherited gravitational faults and how we sampled the material we experimented. Then we present the relation between mechanical and physical parameters and the different processes which influence the mechanical behaviour of the cataclastic material. Afterwards we detail mechanical and physical tests that we performed. Finally, we discuss our results using a physical interpretation. In order to discuss on the variability of the mechanical parameters, we also undertook to study and give the mechanical tests of the fault zone which is not affected by the gravitational phenomenon. To conclude we analysed the space and time evolution of the two principal mechanical parameters.

Landslide study area

Location, geology and geomorphology

The La Clapière landslide is located in the western part of the NW–SE oriented Tinee valley, near Saint-Etienne-de-Tinee (Southern Alps, France, in the Argentera external crystalline massif; Fig. 1).

This deep-seated landslide is bordered at the NW by the Tenibres creek in its northwest and by the Rabuons creek at the south east, both of which flow into the Tinee River, which borders the base of the landslide on a 1.1 km wide distance. The three valleys trend to form a N 010° E prismatic geometry that allows a tri-dimensional view of the unstable area. The elevation of the bottom Tinee valley is 1,100 m (a.s.l.) and the two creeks create a 300-m deep incision in the slope. The La Clapière landslide is part of a massif basal slope which culminates at 2,200 m. Elevations of the surrounding crests and peaks reach 3,000 m. The top of the landslide is a 120-m high head scarp that extends over a width of 800 m at an elevation of 1,600 m. The landslide currently overlaps the Quaternary alluvial deposits of the Tinee River (Jomard 2006).

One of the first studies of the La Clapière landslide was carried out by Follaci et al. (1988). His interpretation of the current landslide explains it as a movement being part of a greater deformation zone and linked to gravitational toppling of the variscan gneisses foliation of the slope.

Julian and Anthony (1996), in agreement with Follaci et al. (1988), relate this gravitational toppling, which seems to be common in the Tinee valley, to a superficial extensive tectonic activity, including a deep crustal scale N 020–030° E compressive regime (Jomard 2006). The combination of tectonic and external solicitations induces superficial stresses on slopes and crests,

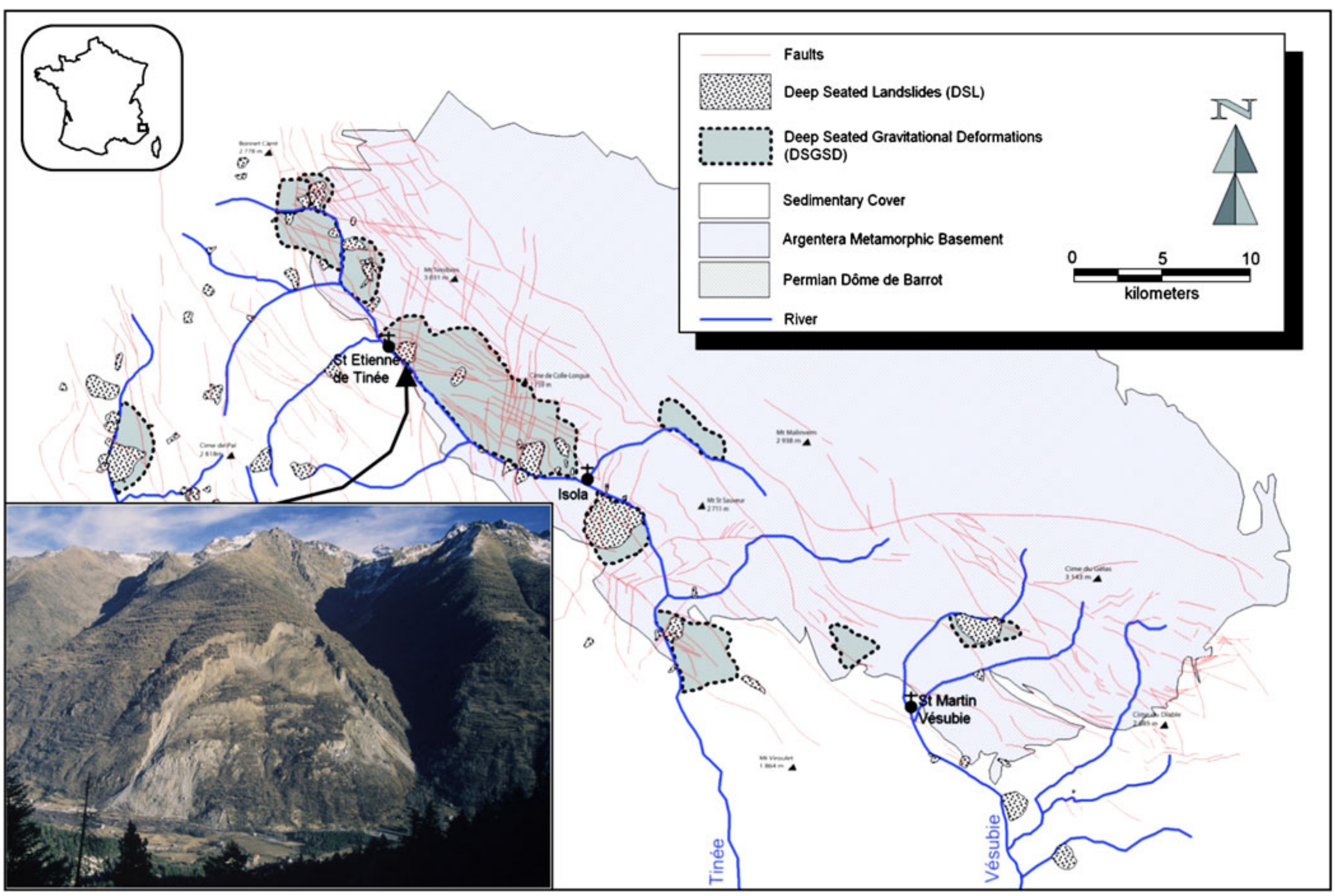

Fig. 1 Localisation of the studied area in the NW–SE oriented Tinee valley, near the Saint-Etienne-de-Tinee village (Southern Alps, France) after Jomard 2006. Localisation of the main faults, the deep-seated landslides, the deep-seated gravitational deformations and the geological formation (sedimentary cover, Argentera metamorphic basement and Permian Dome de Barrot)

which affect pre-existent lineaments. An upwarding evolution of the stress spread and the subsequent instabilities has been observed at the scale of the valley (Jomard 2006). External solicitations are supposed to be mostly linked to glacial debutressing. The importance of the deglaciation is commonly associated to the initiation of gravitational toppling as observed on the La Clapière landslide. Gunzburger and Laumonier (2002) have shown that the origin of rock columns toppling in the La Clapière slope cannot have a single glacial origin. This assumption has been previously confirmed with numerical modelling (Merrien-Soukatchoff et al. 2001).

Cappa et al. (2004), Guglielmi et al. (2005) and Jomard (2006) describe this landslide as a slide fitted into a higher scale movement, characterized by a trench and fracture network, which is inherited via the fault network.

Ivaldi et al. (1991) have shown that the foliation plan's directions into the metamorphic solid mass are different between the La Clapière landslide and the whole solid mass. Near the La Clapière landslide, the foliation plan cuts the rock mass on a macroscopic and a microscopic scale, resulting into a lenticulation. A variation in rock cutting explains a mechanical embrittlement of the zone in the La Clapière landslide area.

In this case, two phenomena may influence the mechanical parameters in opposed ways. The grain elongation of the gneissic material gets more pronounced and the average particle diameter size gets smaller.

Morphology of inherited gravitational faults

From field observations, the tectonically inactive faults reactivation depends mainly on two mechanisms of displacement. The first reactivation mechanism creates the scarps morphology (Fig. 2). It is characterized by a simple unidirectional tangential displacement along the inactive fault combined with a colluvium deposit. The scarps represent the visible part of the collapsed surface. They correspond to extensive movements or secondary landslides (Agliardi et al. 2001).

The second reactivation mechanism creates the trenches morphology (Fig. 2). It gathers a tangential displacement with a rotational movement of the lower part. The active zone is filled with colluviums in association to these displacements. The trenches are most frequently observed in DSGSD (Jahn 1964; McCalpin 1999). Onsite, decametric openings were observed (Cappa et al. 2004; Binet 2006).

Criteria to distinguish tectonic faults from gravitational faults involve to their length, the continuity in number of scarps, their plan shape in relation to the topography, their displacement history (El Bedoui et al. 2009) and the style of deformation (McCalpin 1999; Persaud and Pfiffner 2004).

The trenches and scarps studied are located in the immediate periphery of the La Clapière landslide (Fig. 3). They are deformed and dislocated in the landslide body. The orientations of these structures (fault profiles) follow the N 120° (A and B) and N 40° (C) fracturing network (Fig. 3). The N 120° orientation corresponds to the upper Tinee Valley and the Argentera general orientation (Bogdanoff 1986). It is also perpendicular to the general displacement direction which contributes to the opening of the trenches (Casson et al. 2003). The N 40° structures cut and therefore facilitate the opening of N 120° structures. Onsite, the opening of the trenches and the tangential movement of the scarps are associated to the rock decompression and the slope movement. Zone A presents a different geomorphology from zones B and C. This structure has trench morphology with a large opening. Whereas, zone B is a scarp-oriented N 120°, at a later stage of evolution than zone C-oriented N 40°.

Samples location and description

Samples location

To avoid any contamination by grus and soils, the samples were taken in deep and fresh trenches and scarps crossing the studied faults. The sample zones are indicated on Fig. 3.

One of the major difficulties for this study was the research of sampling zones. The hard accessibility and the small outcrop of the "uncontaminated" cataclastic gneissic material did not permit large samples to be taken. Nevertheless, three zones of shearing A, B and C were defined and sampled, and three zones without landslide shearing D, E and F were defined and sampled (Fig. 3).

- Zones A and B are oriented N 120°, zone C is oriented N 40°, according to Hercynian and Alpine fracturing directions. We choose to carry out a sampling for these three faults from the

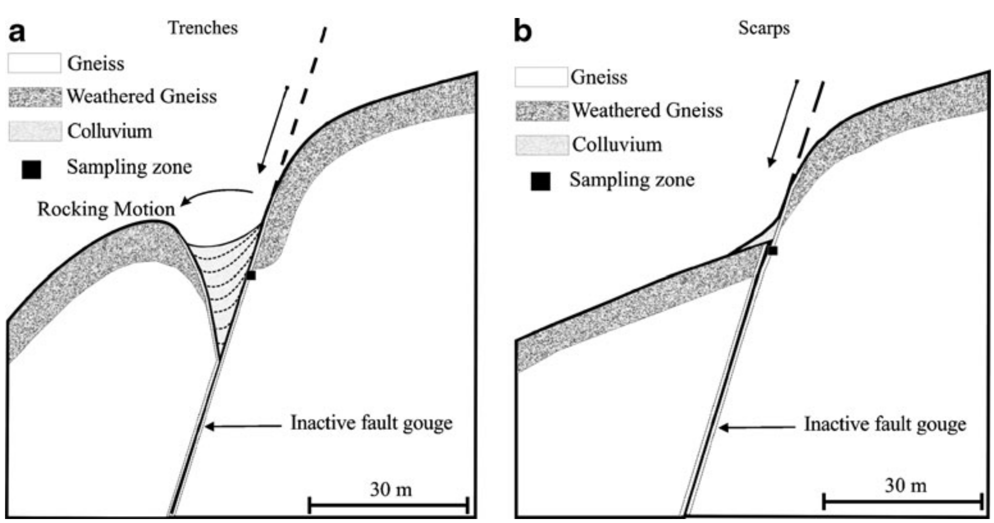

Fig. 2 **a** Schematic representation of the trenches. **b** Schematic representation of the scarps, with the structuration of the gneiss, weathered gneiss and colluviums material

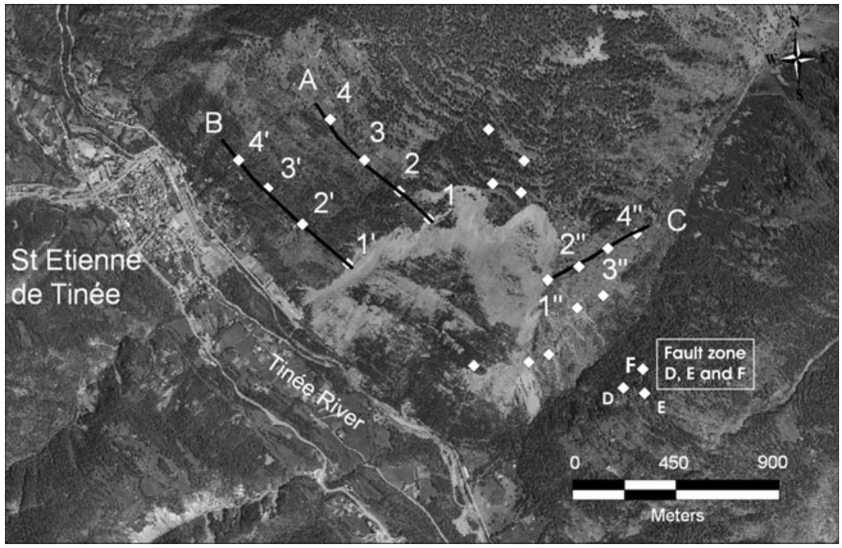

Fig. 3 Mapping of the shearing zones *A*, *B* and *C* (faults segments) and the sampled zones around the "La Clapière" Landslide (zone *D*, *E* and *F*) on aerial photography

zone where the fault is closed again (fault with very little gravitational deformation; A4, B4′ and C4″) to the edge of the slip where the maximum of deformation took place (A1, B1′ and C1″).

- Zones D, E and F are out of the landslide, but in the same tectonical faults than those in the La Clapière landslide. These zones are much closed and are not affected by the landslide. These zones will be our reference frame (non-gravitating) for the cataclastic material resulting from the same fault families as that which take part in the La Clapière landslide.

Samples description

The reactivated faults are located in the Anelle formation which is a migmatitic gneiss rich in biotite and muscovite (Jomard 2006). This formation also contains disthene, sillimanite, garnet and sometimes potassium feldspar (Bogdanoff 1986). In accordance with its definition the gneiss is a banded, coarse-grained rock. During the rock alteration, these grains are separated from the healthy rock and are found to be the deterioration product in faults.

An example of trench and cataclastic material is given in Fig. 4.

These cataclastic materials are composed of discrete particles with more or less regular forms, arranged in a random way. During the evolution of DSGSD zones, the faults are reactivated and the initial cataclastic material contained in the inactive gouge is exposed to several phenomena which modified their mechanical properties.

Methods

In this study as in the previous one (Jomard et al. 2006), based on triaxial tests, we observe mechanical parameters variations along

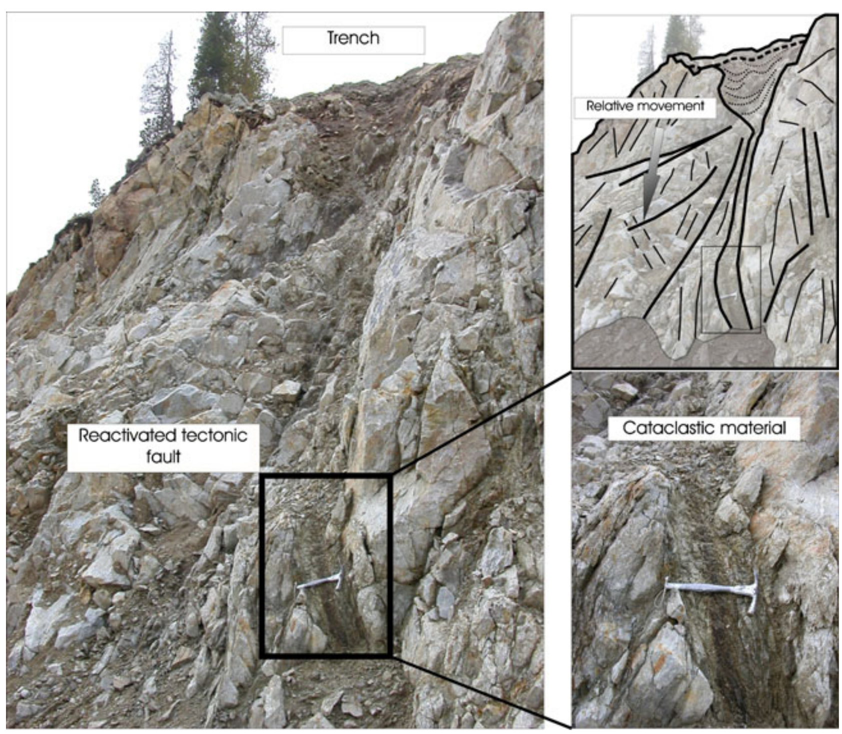

Fig. 4 Photography and schematic explanation of a characteristic trench in the Tinee valley (France)

the reactivated fault. These variations may be explained by three "initial characteristics" and three external processes.

The initial characteristics are:

1. The mineral composition of the parent rock
2. The foliation
3. The primary mechanical characteristics of the gouge

The three external processes are:

1. The tangential displacement
2. The weathering
3. The leaching

In order to highlight, which initial characteristic or which external processes dominates the others, we complete the triaxial tests (mechanical parameters) with particle size distribution tests (physical parameters). To summarize, the initial characteristic and the external processes influence the physical parameters which themselves condition the mechanical parameters. In this paragraph, we first recapitulate the well-known relations between physical parameters and mechanical parameters. Then, we describe initial characteristics and external processes and their influence on the mechanical parameters.

The internal variability of φ' and c' is mainly controlled by the shape and the particle size distribution (Morris 1959; Frederick 1960; Zelasko 1966; Frossard 1979; De Jaeger 1991; Chan Tien 1998). At the scale of the samples, φ' is conditioned by the granular skeleton and c' by the matrix (Lebourg 2000; Lebourg et al. 2003, 2004). The variations of the mechanical parameters can be resumed:

- φ' increases according to a particle roughness or elongation increasing
- For a constant compaction, φ' increase according to an average particle diameter or a grading increasing
- c' increase with the proportion clay in the matrix

The three initial characteristics may influence the mechanical behaviour in opposite ways: φ' and c' may increase or decrease.

Triaxial test

Because of the nature of the samples and according to our hypotheses, triaxial compression tests were carried out. Within the framework of this study, gneissic material has a drained behaviour whatever the stress application conditions can be. Interstitial overpressures being insignificant, the applied stress is completely transmitted to the solid skeleton and becomes the effective stress. For each sample, four tests were performed, with consolidation and drainage (CD tests), at 100, 200, 300 and 400 kPa for a 25% maximum deformation and for 3 mm/mn compression velocity. The effective angle of internal friction (φ' in degree) and the effective cohesion (c' in kPa) are calculated using the method of the least rectangles (Dagnelie 1998) and according to the well-known relations of Terzaghi (1967). These parameters are classically used in the equation of the Mohr–Coulomb failure criterion:

$$\tau_{\max} = c' + \sigma_N' \times \tan \varphi', \qquad (1)$$

where $\tau_{\max}$ is the maximum shearing stress and σ_N the normal stress (Costet and Sanglerat 1981).

In order to detect small parameter variation, a careful protocol for the triaxial compression tests has been realized.

Particle size distribution tests

The experimental protocol is officially defined according to the recommendations of the French standards related to the particle size distribution analysis (P18–560 Normes Françaises (1994)). Such standard grain size distribution analyses were performed on all the samples coming from the three shearing zones A, B and C. The grain size distribution analysis measures the mass grade ratio of gneiss components. The granulometric size classes are defined by the size of sieve meshes (Normes Françaises—P18–560 1994) and from the clays (Ø<2 mm) to the metric blocks and sometimes decametric blocks. The granularity is one of the particle soil properties defined by combination of the decile (*C*%) grain size curve:

Cu: uniformity coefficient or Hazen coefficient: Cu, with Cu= *D*60/*D*10: Cu characterizes the grain size curve dispersion, with for Cu (sand, 1.4; river deposits, 0.8; slopes debris, 41 and tills from 10 to 150)

Sk1: the coefficient of Ward, called asymmetric coefficient define by Folk and Ward (1957) with $Sk_I = \frac{\Phi_{16}+\Phi_{84}-\Phi_{50}}{2(\Phi_{84}-\Phi_{16})} + \frac{\Phi_5+\Phi_{95}-2\Phi_{50}}{2(\Phi_{95}-\Phi_5)}$,The coefficient of Folk and Ward (Ski), makes it possible to measure the degree of asymmetry of a granulometric function, with a finer precision and a better discrimination of materials (Table 1), with for Ski (sand, 0.08; alluvions, 0.001; slopes debris, 0.1 and tills from 0.1 to 0.5)

Cc: the curvature coefficient: Cc=$(D30)^2/(D10\times D60)$, (Table 1), with for Cc (sand, 0.7; Alluvions, 1.1; slopes debris, 3.1 and tills from 0.6 to 5.9), (Lebourg et al. 2003)

Table 1 Grain size distribution parameters (Cu, uniformity coefficient; Sk1, the coefficient of Ward; Cc, the curvature coefficient and the clay content %)

	A1	A2	A3	A4	B1′	B2′	B3′	B4′	C1″	C2″	C3″	C4″
Cu	26.9	26.5	77.6	29.5	29.6	30.8	25.6	33.7	5.9	8.7	4.1	10.8
Ski	0.68	0.48	0.11	0.73	0.82	0.82	0.90	0.84	0.70	0.75	0.79	0.47
Cc	0.62	1.22	3.24	0.33	0.19	0.21	0.32	0.24	0.95	1.15	0.78	0.81
Clay %	4	7.1	10.7	12.9	6.1	8.9	15.5	25.2	3.1	9.5	12.3	16.4

The various granulometric parameters defined describe the general aspect of the sample, in this case, a wide range of grain size, a low frequency of finest elements (Ø<0.08 mm, limit of the silts) and a high frequency of grains with a diameter Ø>2 mm (Table 1). Each granulometric grain size class is quantified and characterized through shape and size parameters, which then allows us to classify and characterize the gneiss weathered material.

Previous study and state of art

Primary mechanical characteristics of the gouge

A mechanical behaviour may come from the inherited tectonic activity. Early stages of fault core formation are mainly dominated by particle fragmentation while particle abrasion controls the distribution of particle size and shape in fault gouge (Storti et al. 2003). The first mechanism is mainly related to the state of stress within the deforming cataclastic rocks, while particle crunching essentially depends on slip-enhanced rolling and shearing. Both mechanisms likely determine the evolution of particle size distributions in shear bands. The shearing and the weathering have a similar effect on the cataclastic material than the "actual" tangential displacement and weatherings of the reactivated fault (see part 3.3.2 and Fig. 5).

External process and mechanical parameters

In this part, we describe the distribution of the external processes along the discontinuities and their influence on the mechanical parameters of the cataclastic material.

Cappa et al. (2004) wrote that the La Clapière landslide can be taken as a highly permeable fractured reservoir because of large pores inside opened fractures, breccias and blocks formed by the displacements. The opening and the healthy rock destructuring along the reactivated faults are increasingly important towards the La Clapière landslide (Jomard 2006; Tric et al. 2010). Consequently, the surface exposed to the drainage of the meteoric water gets increasingly important. The external processes like weathering and leaching are accentuated with the increasing intensity of the drainage. In this configuration, it is supposed, that the leaching and the weathering from the healthy area to the landslide increase.

The geomorphological study indicates that the A reactivated fault has a larger drainage surface than B, and B a larger surface than C. Hence, the faults A, B and C are respectively increasingly exposed to the leaching and the weathering processes. For the faults D, E and F, they are not open and very low affected by weathering.

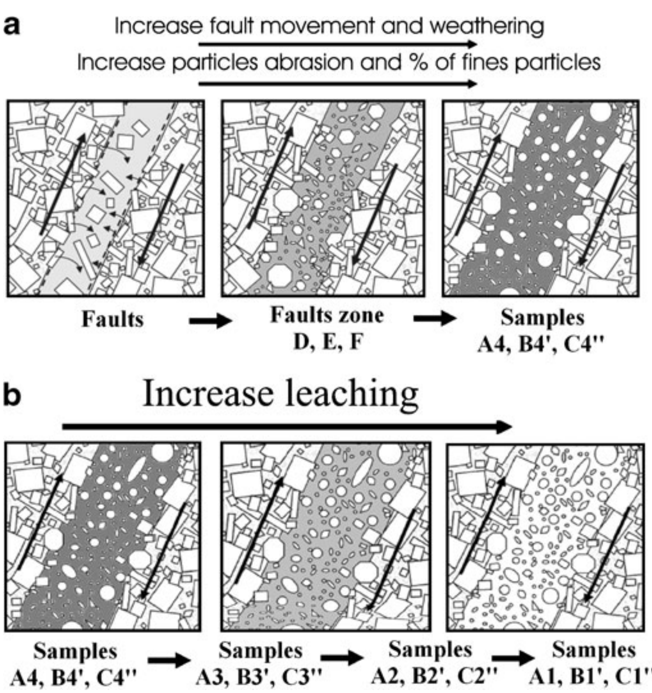

Fig. 5 The *different shades of grey* illustrate the content of fines in the material, by using darker colour for higher percentage (not to scale). This figure is a simple example of the three processes which are active in the reactivated fault; **a** the increase of mechanical crunching and weathering with the increase of displacement, and **b** the increase of leaching with the increase of displacement

Tangential displacement and weathering: φ' decreasing and c' increasing

The tangential displacement and the weathering decrease grading and diameter average of the particles. The shearing increases the particles crunching (Fig. 5) and strongly modifies their stress–strain behaviour, strength and compressibility (Hardin 1985; Fukumoto 1992; McDowell and Bolton 1998; Storti et al. 2003).

The weathering strongly affects crystalline rocks (Lumb 1962; Onodera et al. 1974; Howat 1985; Arel and Tugrul 2001; Kim and Park 2003; Borrelli et al. 2007). In gouge fault, intense weathering conditions (Fig. 5) determine reductions in shear strength (Jaboyedoff et al. 2004). The weathering products of gneiss are kaolinite, halloysite and Fe-oxides (Critelli et al. 1991). Finally, the increasing of the clay ratio accentuates the material cohesion.

Leaching process: φ' increasing and c' decreasing

The finest particle leaching (Fig. 5) indirectly influences the mechanical parameters. The hydrolysis of gneiss leads progressively to the destruction of phyllosilicates and the feldspar (Le Pera et al. 2001). The quartz ratio in the matrix, the contact between grains, the grading and the average particle diameter are increased as the resulting clays are drained by infiltrating water (Jomard et al. 2006).

The tangential displacement and weathering (φ' decreasing and c' increasing) processes compete against the leaching process (φ' increasing and c' decreasing) along the reactivated faults.

Results

We carried out triaxial compression tests on two types of faults: the La Clapière gravitational faults (segment faults A, B and C) and non-gravitational faults which are close to La Clapière but which was not included in the destructuration of the landslide (faults D, E and F). The objectives are to compare the various evolutions between faults which do not have the same history and thus to propose a quantification of the effect to the process of shearing and effects of the weathering of a gravitational faults since the beginning of the landslide activity of the La Clapière.

Mineral composition of the parent rock and grain size distribution tests

The six faults (three gravitational faults (A, B and C) and three non-gravitational faults (D, E and F)) are in the same geological formation (Anelle formation) described in the geological setting. However, the ratio, the size and the morphology of the mineral included in the matrix of the parent rock can fluctuate in the space. The gouge material is clearly stemming from the mechanical desegregation of these minerals (Fig. 5). Hence, the different size and morphology can be found again in the cataclastic material and influence its mechanical behaviour.

Grain size distribution results have shown that most conventional parameters (Cu, Cc and Ski, see particle size distribution tests section, Table 1) did not show a significant change, except for values content of fine particles. Indeed, we observe that the further away from the drainage area over the content of fine elements increases. This result is consistent with the idea of the role of the proposed leaching phenomenon.

Triaxial test results of the weathered gneiss in the gravitational faults and non-gravitational faults

Measurements of the effective angle of internal friction (φ') are represented in Fig. 7 as a function of the effective cohesion (c'). On the whole, φ' decreases slightly when c' increases.

For the gravitational faults (faults A, B and C):

- The internal angle of friction: φ' values are included between 32.6±0.5° and 24.7±0.3°. The A and B zones have quasi similar φ' values for the points groups (1, 1′), (2, 2′), (3, 3′) and (4, 4′), whereas these values are different for the C zone (1″, 2″, 3″ and 4″) except for the plot 2″.
- The cohesion: c' values are included between 0±2 kPa to 36±2 kPa. The A and B zones have also close c' values for the points groups (1, 1′), (3, 3′) and (4, 4′). Points 2 and 2′ of c' values are more distant than their φ' values. Points 2″ and 4″ of the C zone are located apart from the other zones.

The A and B zones show approximately similar tendencies whereas C zone can be distinguished in the φ' domain by lower values.

For the non-gravitational faults (D, E and F):

- The internal angle of friction: φ' values are included between 26.5±0.5° and 27.6±0.3°, with an average of 27±0.6°
- The cohesion: c' values are included between 31±2 kPa to 45±3 kPa, with an average of 38±6 kPa

The faults D, E and F zones show tendencies higher than all the zones study for the gravitational areas, only the sample of area C4″ is similar.

Mechanical parameters variations may as well be related to their distance from the landslide. The effective angle of internal friction and the effective cohesion are plotted as a function of distance to the landslide in Fig. 7. Measured data are represented on these graphs.

Figure 7 displays a general slight diminution of the effective angle of internal friction when the distance to the landslide increases.

On the contrary, Fig. 7 displays a general increase of the effective cohesion when the distance to the landslide increases. This increase is more distinct than the internal angle of friction diminution

Discussion

Mechanical analysis of the gravitational faults

On Fig. 6, three groups of points can be distinguished: neighbouring points groups (1, 1′, 1″), (2, 3, 4, 2′, 3′, 4′) and a scattered points group (2″, 3″, 4″). These groups are coherent with the points' geographical settings. The first group is significantly separated from the others. Corresponding samples are located to the closest of the La Clapière landslide body. The samples of the

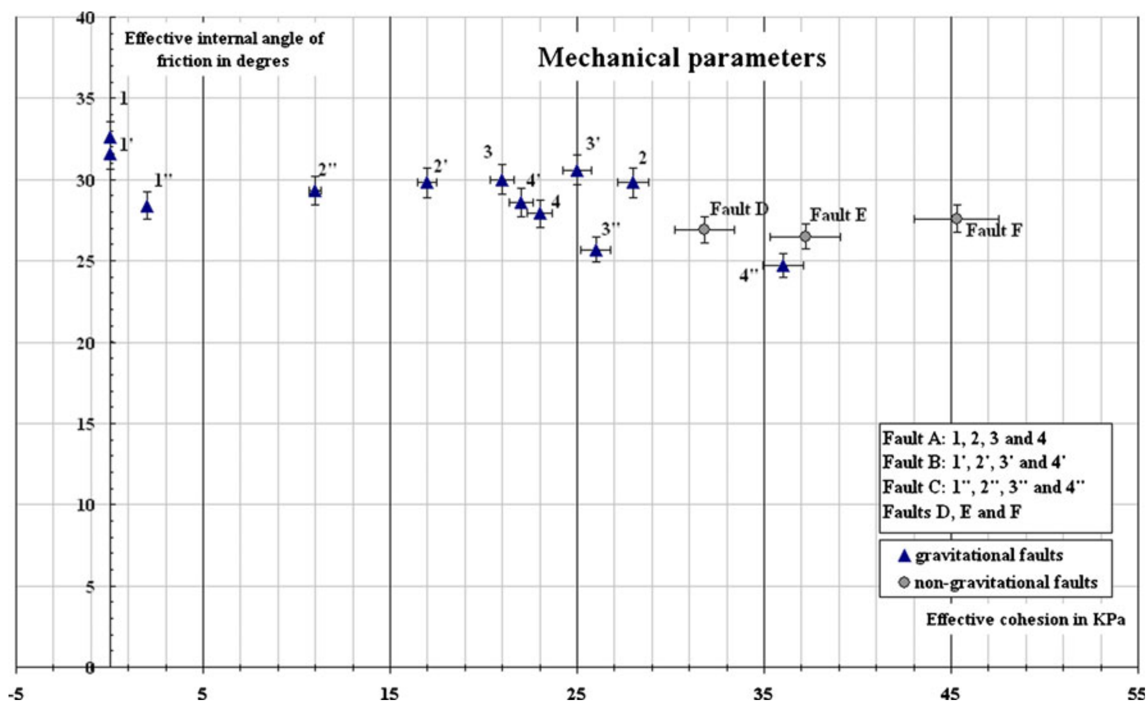

Fig. 6 Mechanical parameters distribution of gravitational fault samples and non-gravitational faults samples (with the effective cohesion (c') in kilopascal and the effective angle of friction (φ') in degree)

second group are situated in the same geographical zone, on the same slope and with the same reactivated fault orientation. The third group of samples is located along the zone C.

The Fig. 7 shows a slight diminution of φ'. However, this diminution may be covered by uncertainties. On the contrary, Fig. 7 displays a general increase of the effective cohesion with increasing distance to the landslide. In a global view, the triaxial results confirm that the observations made by Jomard et al. (2006), c' decreases and φ' increases from the unweathered area to the weathered area.

This mechanical evolution cannot be explained by the tangential displacement and the weathering which should have an opposite effect along these reactivated faults. On the other hand, this variation may be explained by the leaching, the initial characteristics of the material or a combination of both. This leaching could be also explained by the opening of the gravitational trenches since the beginning of the La Clapiere landslide 3.6 ka ago (Bigot-Cormier et al. 2005; El Bedoui et al. 2009) (Fig. 8).

Indeed, in his research El Bedoui (Fig. 8) showed three phases of the deformation of the landslide guided by these gravitational faults, and this at three different scale time: (1) step 1 with an initial slow

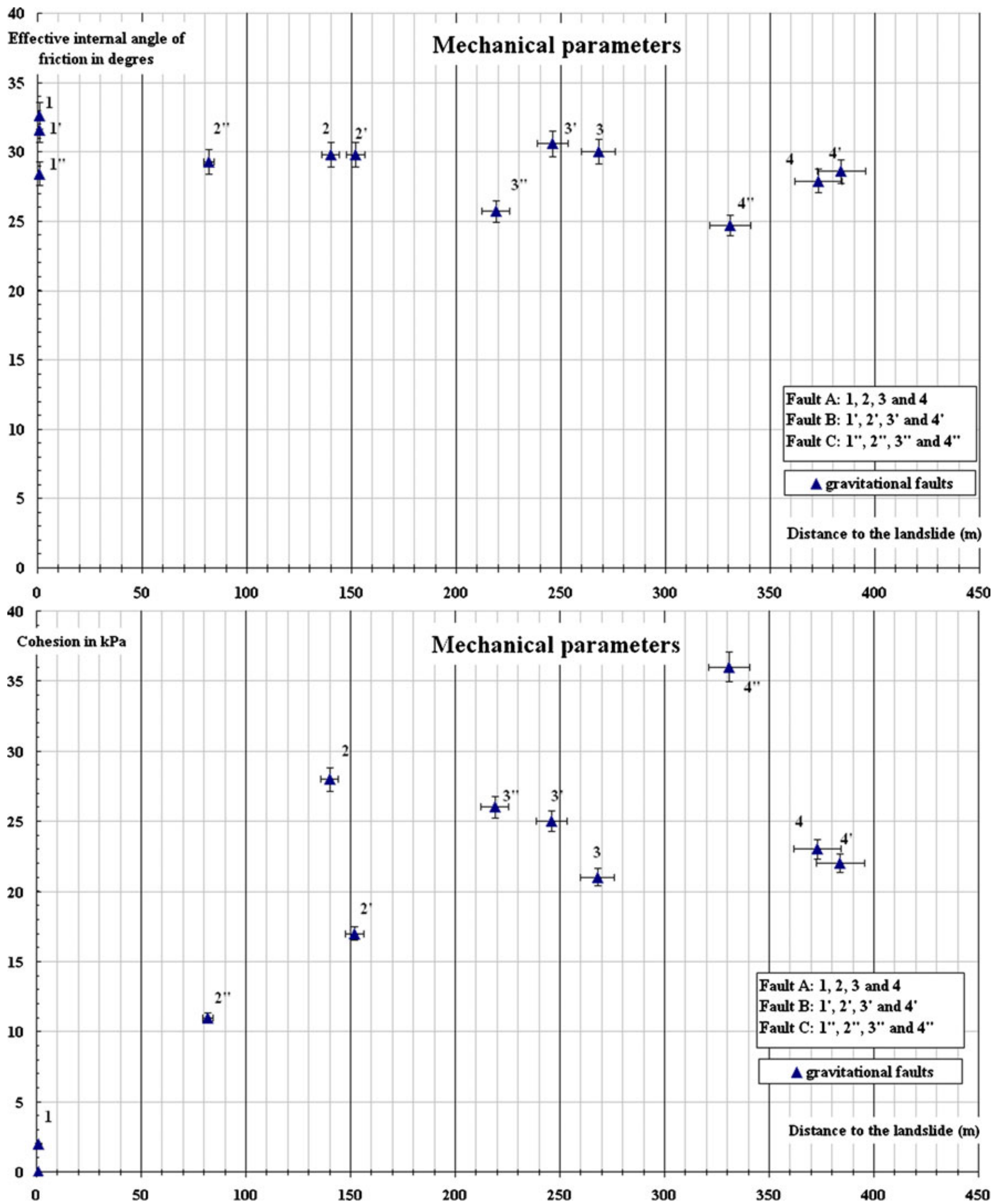

Fig. 7 Effective angle of internal friction (φ') in degree versus distance to the landslide and the effective cohesion (c') in kilopascal versus distance to the landslide

Fig. 8 Reconstruct paleo-slope geometry of the La Clapiere landslide (in el Bedoui et al. 2009); reconstitution of the progressive surface shearing since 3.6 ka BP and the La Clapière slope velocity for the last 10 ka

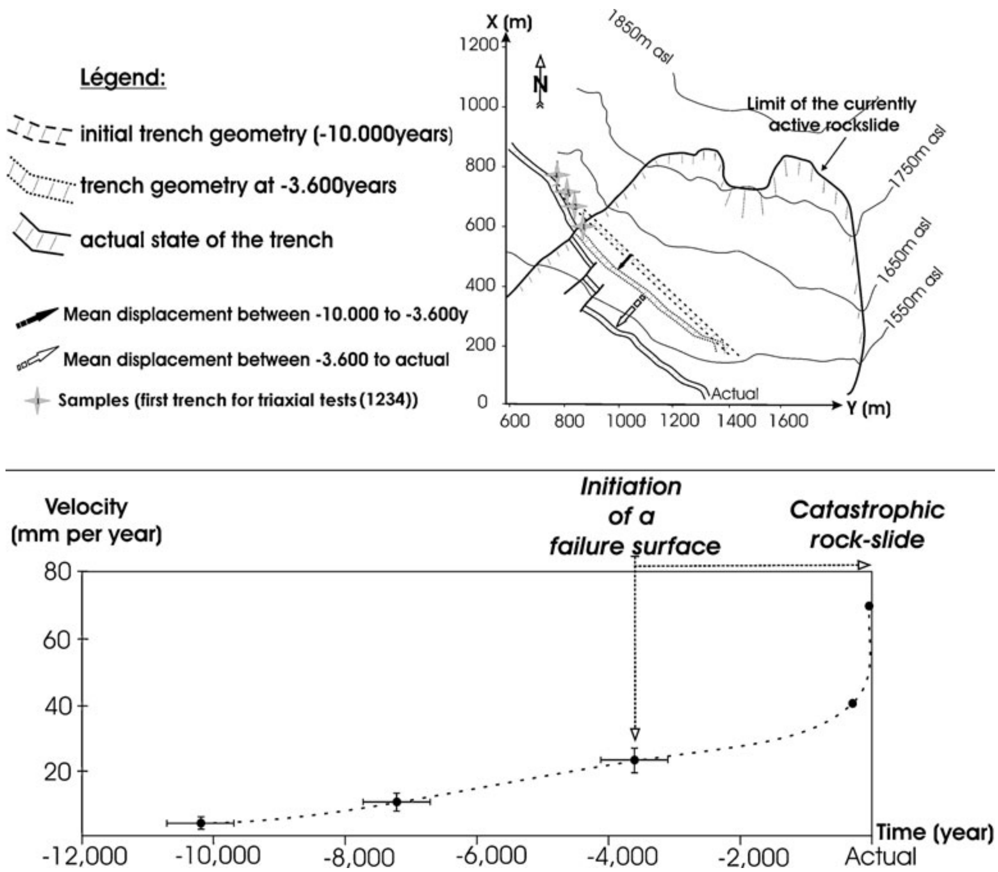

slope deformation, spreading from the foot to the top, characterized by an average displacement rate of 4 mmyear^{-1}, from 10–5.6 kaBP; (2) step 2 with an increase in the average displacement rate from 13 to 30 mmyear^{-1} from the foot to the middle of the slope, until 3.6 kaBP and (3) step 3 with the development of a large failure at the foot of the slope with fast displacement rates exceeding 80 mmyear^{-1} for the last 50 years. During the different phases the failure developed slowly from the foot to the top, explaining the extensive occurrence at the surface of morphostructural features (trenches, counters scarps and double ridges). Before the rock slide was triggered, the slope was cut by two families of inherited discontinuities (faults A, B and C). Several discontinuities were reactivated and then generated the formation of the trenches. During the slow evolution of the slope (phase I and the beginning of phase II), the internal rock mass damage did not change a lot the mechanical parameters (areas A4, B4′ and C4″ with similarity with faults zone D, E and F), and during the third phase (3.6 ka BP) the gravitational faults starts opening with the beginning of weathering and leaching processes.

If we propose the following assumptions:

- Beginning of the La Clapière landslide at 3.6 ka BP (Bigot-Cormier et al. 2005; El Bedoui et al. 2009)
- The opening in traction of the gravitational faults since the landslide towards the outside of the landslide (of 1 towards 4) (Jomard et al. 2006, 2010; El Bedoui et al. 2009),
- Beginning of weathering and leaching processes,
- An opening in traction with a linear evolution which can allow us to extrapolate the opening of the trenches from zones (A1, B1′ and C1″ since 3,600 years) to now with trenches (A4, B4′ and C4″ at medium distance of 370 m from the landslide).

If we consider that zones A4, B4′ and C4″ (with an average value of $\varphi'=27.06° \pm 0.8°$, and $c'=27 \pm 3$ kPa, Fig. 9) correspond to the gravitational fault in its original state dated at 3.6 ka BP and the zones A1, B1′ and C1″ (with an average value of $\varphi'=30.8° \pm 0.9°$, and $c'=0.6 \pm 0.6$ kPa, Fig. 9) close to La Clapiere landslide correspond to the faults at time present, we obtain Fig. 9 which present the temporal evolution of φ' and c' since 3,600 years.

For both mechanical parameters (φ' and c'), we observe a very simple behaviour (Fig. 9):

- In case of the internal angle of friction, this behaviour is clearly linear and the following "time law" of increasing of the internal angle of friction can be proposed

$$\varphi'_t = 27.26 + 1.74 \times 10^{-3} y, \qquad \text{(Fig. 9)}, \qquad (2)$$

where φ' is the internal angle of friction n years after the beginning of the landslide process and y the number of years (n years) after the landslide beginning. This law correspond to an increasing of the internal angle of friction of 1.7° (±0.4°) each thousand years.

If we apply the same consideration to the cohesion c', we observe a behaviour slightly different, either linear or polynomial:

- The linear behaviour gives the following law:

$$c'_t = 30.2 - -7.6 \times 10^{-3} y, \qquad \text{(Fig. 9)}, \qquad (3)$$

which correspond of a decreasing of the cohesion of 7.6 kPa (±2 kPa) each thousand years, with c'_t the cohesion n years after the beginning of the landslide process and y the number of years (n years) after the landslide beginning.

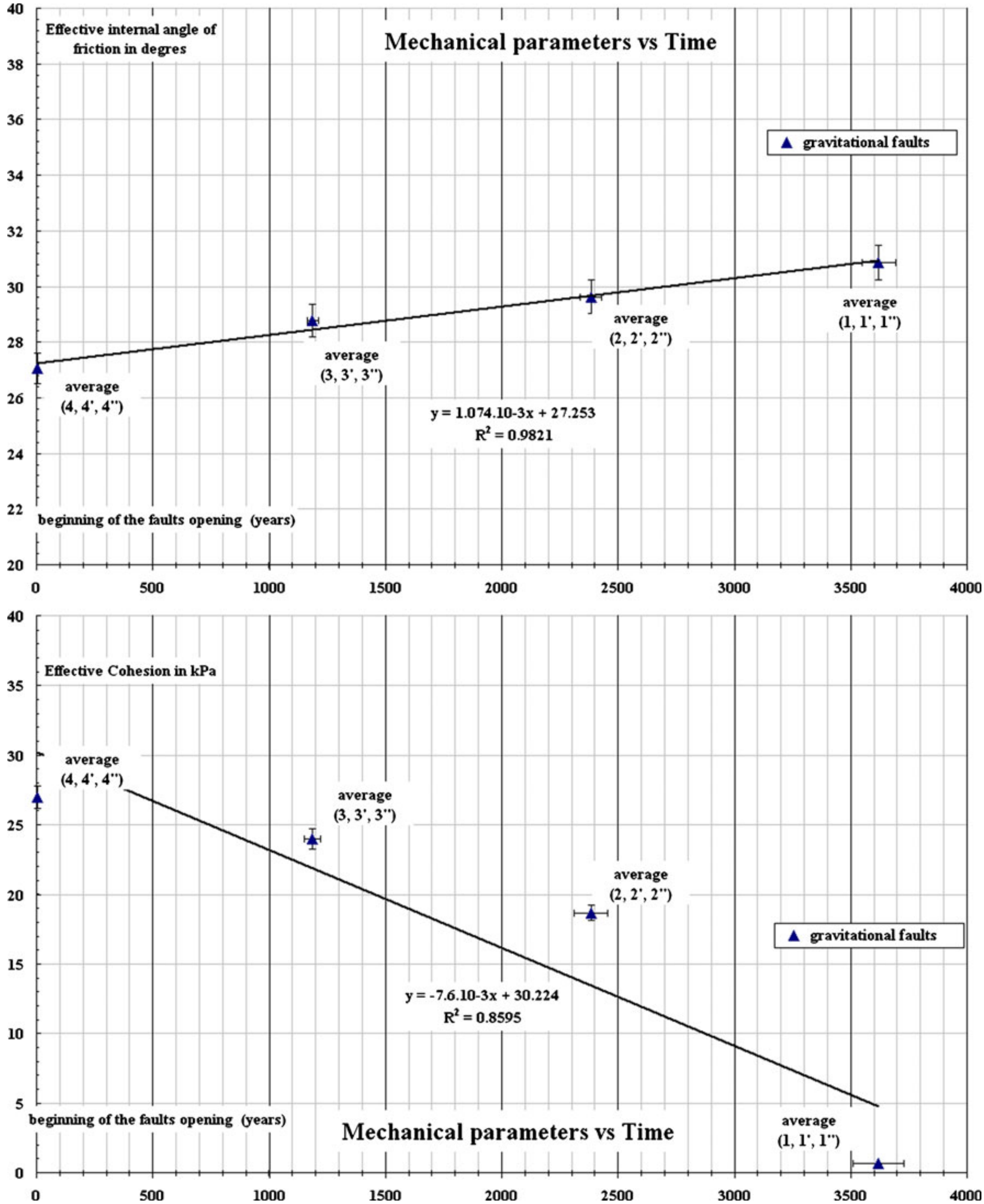

Fig. 9 Time evolution of the effective internal angle of friction (φ') in degree and the effective cohesion (c') in kilopascal of the la Clapière landslide since 3,600 years

– The polynomial behaviour gives the following law:

$$c_t^{'} = -3.0 \times 10^{-6} y^2 + 0.0021y + 26.497 \qquad \text{(Fig. 9)} \qquad (4)$$

Proposition of an interpretation of the spatial evolution of the mechanical parameters

The cataclastic material embedded in the inherited faults can be considered as a lubricant in the rock which facilitates the accommodation of stresses and strains. These planes of weakness in the gneissic rock are remobilised according to gravitational stresses in high mountain rock causing the cataclastic material to be affected by a "gravitational crunching".

The mechanical and physical parameters obtained in this study could be considered as indicators of the degree of deterioration resulting from the mechanical and chemical weathering and from the gravitational crunching of inherited tectonic faults. Onsite, displacement on gravitational faults is increasingly important toward the La Clapière landslide. The overlapping of the gravitational crunching on the cataclastic material and the chemical weathering, especially the hydrolysis of the silicate, create finest elements from silts to clay. The expected results were a degradation of the grains, a decrease of φ' and an increase of c'.

However, along the three gravitational faults studied (A, B and C, Fig. 3), the triaxial test results show that φ' tends to increase near the landslide, whereas the values of c' clearly decrease. For each shear zone, with a precision less than φ' and c', the whole grain size distribution indicates that more the shear zone is open or developed; more the residual material loses its finest particles.

The influence of the drainage in these zones explained by the opening of the La Clapiere landslide since 3.6 ka BP is a determining factor to explain the results obtained. The leaching of the finest particles increases with the opening of the gravitational faults and the rock decompression, and therefore acts on the mechanical behaviour. Moreover, the leaching may explain the poor concentration of silt inside our samples. The zone C seems to be less affected by the leaching.

Conclusion

This study was realised in order to increase the understanding of the mechanical repartition of the cataclastic material along a gravitational reactivated faults. The sampling was performed in six faults, three gravitational faults taking part in the La Clapiere landslide and three faults close to the landslide, but not reactivated. Measures for the φ' and c' were analysed along the reactivated fault in order to quantify the evolution in space and in time of the mechanical behaviour. The analysis shows a real change of the mechanical properties along the three gravitating faults. They highlight a modification related to the leaching of these faults which has been synchronous with the deformation of the La Clapiere landslide for 3,600 years. In our paper, we have made the assumption that these faults had been in opening for 3,600 years and mechanical analysis of the cataclastic material of the studied fault (zones A4, B4′ and C4″) had the equivalent properties that the non-gravitational faults (zones D, F and E, Fig. 3). Upon the basis of these observations, we propose to explain the change of the mechanical properties of the gravitating faults by a phenomenon of leaching and weathering. During the third phase from 3.6 ka BP to now, we observe a development of a large failure at the foot of the slope with fast displacement rates and development of extensive occurrence at the surface of morphostructural features (trenches and counters scarps). If we admit the assumptions of the beginning of the Clapière landslide at 3.6 ka BP, the opening in traction of the gravitational faults since the landslide towards the outside of the landslide (of A1 towards A4, B1′ towards B4′ and C1″ towards C4″), with the beginning of weathering and leaching processes, we can propose to explain and quantify the mechanical by a relative increasing of the angle of friction because of the loss of the finest particles and a relative decreasing of the cohesion.

According to the datings obtained by ^{10}Be which made it possible to know the time of opening in traction of the faults, we propose for the first time two temporal experimental laws of evolution of the mechanical properties from gneissic materials: one time law of increasing of the internal angle of friction with ($\varphi'_t = 27.26 + 1.74 \times 10^{-3} y$; Fig. 9), which correspond to an increasing of the internal angle of friction of 1.7° (±0.4) each thousand years, and a second time law with decreasing of the cohesion.

We are well aware that these laws are specific to the La Clapière site, but they permit to the first time to quantify the temporal dependency of the weathered gneisses. They make it possible to propose the assumption of a significant modification of the mechanical properties according to the maturation of the slopes and the landslides, since a solid mass fractured towards a deep-seated landslide (La Clapiere), but also to quantify in time the mechanical decrease of the cataclastic zones. Now, these laws of c' and φ' will permit us to constrain the numerical codes which simulate the effect of weathering on the instability processes for La Clapière landslide.

Acknowledgements

This work is supported by the PACA Region, the GIS CURARE Project and the INSU OMIV project (Landslides French Observatory).

References

Agliardi F, Crosta GB, Zanchi A (2001) Structural constraints on deep-seated slope deformation kinematics. Eng Geol 59:83–102

Arel E, Tugrul A (2001) Weathering and its relation to geomechanical properties of Cavusbasi granitic rocks in northwestern Turkey. Bull Eng Geol Environ 60:123–133

Bogdanoff S (1986) Evolution de la partie occidentale du massif cristallin externe de l'Argentera. Place dans l'arc alpin. Géologie de la France 4:433–453

Bigot-Cormier F, Braucher R, Bourlès D, Guglielmi Y, Dubar M, Stéphan JF (2005) Chronological constraints on processes leading to large active landslides. Earth Planet Sci Lett 235:141–150

Binet S (2006) L'hydrochimie, marqueur de l'évolution a long terme des versants montagneux fractures vers de grands mouvements de terrain. PhD Thesis 190

Borrelli L, Greco R, Gullà G (2007) Weathering grade of rock masses as a predisposing factor to slope instabilities: reconnaissance and control procedures. Geomorpholy 87:158–175

Cappa F, Guglielmi Y, Soukatchoff VM, Mudry J, Bertrand C, Charmoille A (2004) Hydromechanical modeling of a large moving rock slope inferred from slope levelling coupled to spring long-term hydrochemical monitoring: example of the La Clapiere landslide (Southern Alps, France). J Hydrol 291:67–90

Cascini L, Critelli S, Di Nocera S, Gullà G, Matano F (1992) Weathering grades and landslides in the gneisses of Sila Massif: the case of S. Pietro in Guarano (Cosenza) (in Italian). Geol Appl Idrogeol 27:49–76

Casson B, Delacourt C, Baratoux D, Allemand (2003) Seventeen years of the "la Clapiere" landslide evolution analysed from ortho-rectified aerial photographs. Eng Geol 68:123–139

Chan Tien CE (1998) Simulation numérique du comportement d'un film granulaire cisaillé en fonction de la rugosité des parois et de la forme des granules. PhD Thesis Lyon 202

Costet J, Sanglerat G (1981) Cours pratique de mécanique des sols. Dunod, p 630

Critelli S, Di Nocera S, Le Pera E (1991) Approccio metodologico per la valutazione petrografica del grado di alterazione degli gneiss del Massiccio Silano _Calabria setten-trionale. Geol Appl Idrogeol 26:41–70

Dagnelie P (1998) Statistique, theorique et appliquees. Statistique descriptive et bases de l'inference statistique. De Boeck, Universite, Paris, Bruxelles, pp 1–499

De Jaeger (1991) Influence de la morphologie des sables sur leur comportement mécanique. Univ. Catho. De Louvain, PhD Thesis 3 parts

Durville JL, Lacube J (1992) Mécanisme et modèles de comportement de grands mouvements. Bull Inter Ass Eng Geol 45:25–42

El Bedoui S, Guglielmi Y, Lebourg T, Perez JL (2009) Deep-seated failure in fractured rock over 10.000 years; the La Clapiere slope, the south-eastern Alps. Geomorphology 105:232–238

Follaci JP, Guardia P, Ivaldi JP (1988) Geodynamic framework of "La Clapière" landslide (Maritime Alps, France) (In French). Proc 5th International Symposium on Landslides, Lausanne 2 Publ Rotterdam: A A Balkema 1323–1327

Folk RL, Ward WC (1957) Brazos river bar, a study in the signifiance of grain size parameters. J Sedim Petrol 27:3–27

Frederick MR (1960) An investigation of the effects of particle shape on the shearing resistance of sand. M.C. Project Report, Found. Eng., University Birmingham
Frossard E (1979) Effect of sand grain shape on interparticle friction; indirect measurement by Rowe's stress dilatancy theory. Geotechnique 29:341–350
Fukumoto T (1992) Particle breakage characteristics of granular soils. Soils Found 32 (1):26–40
Gerber E, Scheidegger AE (1969) Stress-induced weathering of rock masses. Eclogae Geol Helv 62:401–415
Guglielmi Y, Vengeon J, Bertrand C, Mudry J, Follaci J, Giraud A (2002) Hydrogeochemistry: an investigation tool to evaluate infiltration into large moving rock masses (case study of La Clapière and Séchilienne alpine landslides). Bull Eng Geol Environ 21(4):311–324
Guglielmi Y, Cappa F, Binet S (2005) Coupling between hydrogeology and deformation of mountainous rock slopes: insights from La Clapière area (southern Alps, France). Comptes Rendus Geosciences 337:1154–1163
Gunzburger Y, Laumonier B (2002) A tectonic origin for the fold underlying the Clapiere landslide (NW Argentera-Mercantour massif, Southern Alps, France) deduced from an analysis of fractures. Comptes Rendus Geosciences 334:415–422
Hardin B (1985) Crushing of soil particles. J Geotech Eng 111(10):1177–1192
Howat MD (1985) Completely weathered granite—soil or rock? Q J Eng Geol 18:199–206
Ivaldi JP, Guardia P, Follaci JP, Terramorsi S (1991) Plis de couverture en échelon et failles de second ordre associes à un décrochement dextre de socle sur le bord nord-ouest de l'Argentera (Alpes-Maritimes, France), C. R. Acad Sci Paris 313:361–368
Jaboyedoff M, Baillifard F, Bardou E, Girod F (2004) The effect of weathering on Alpine rock instability. Q J Eng Geol Hydrogeol 37(2):95–103
Jahn A (1964) Slopes morphological feature resulting from gravitation. Z Geomorph Suppl 5:59–72
Jomard H (2006) Analyse multi échelles des déformations gravitaires du massif de l'argentera mercantour (In french). PhD Thesis 246
Jomard H, Lebourg T, Tric E (2006) Identification of the gravitational boundary in weathered gneiss by geophysical survey: La Clapière landslide (France). J Appl Geophys 62:47–57
Jomard H, Lebourg T, Guglielmi Y, Tric E (2010) Electrical imaging of sliding geometry and fluids associated with deep seated landslide (La Clapiere, France). Earth Surf Process Land 35(5):588–599
Julian M, Anthony E (1996) Aspects of landslide activity in the Mercantour Massif and the French Riviera, south-eastern France. Geomorphology 15:275–289
Kim S, Park H (2003) The relationship between physical and chemical weathering indices of granites around Seoul, Korea. Bull Eng Geol Environ 62:207–212
Lebourg T (2000) Analyse géologique et mécanique de glissement de terrain dans des moraines des Pyrénées centrales et occidentales (France) (In French). PhD Thesis. Bordeaux I 369
Lebourg T, Riss J, Fabre R, Clement B (2003) Morphological characteristics of till formations in relation with mechanical parameters. Math Geol 35(7):835–852
Lebourg T, Riss J, Pirard E (2004) Influence of morphological characteristics of heterogeneous moraine formations on their mechanical behaviour using image and statistical analysis. Eng Geol 73:37–50
Le Pera E, Critelli S, Sorriso-Valvo M (2001) Weathering of gneiss in Calabria, Southern Italy. Catena 42:1–15
Lumb P (1962) The proprieties of decomposed granite. Geotechnique 12:226–243
McCalpin JP (1999) Criteria for determining the seismic significance of Sackungen and other scarplike landforms in mountainous regions. In Techniques for identifying faults and determining their origins, U.S. Nuclear Regulatory commission, NUREG/CR-5503 Appendix A, 122–142
McDowell GR, Bolton MD (1998) On the micromechanics of crushable aggregates. Geotechnique 48(5):667–679
Merrien-Soukatchoff V, Quenot X, Guglielmi Y (2001) Modélisation par éléments distincts du phénomène de fauchage gravitaire. Application au glissement de la Clapière (Saint-Etienne de Tinée, Alpes Maritimes). Rev Fr Géotech 95–96:133–141
Morris HC (1959) The effect of particle shape and texture on the strenght of a noncohesive aggregate. Thesis Washington University
Normes Francaises NF P 94-056 and NF P 94-040 (1994)
Onodera TF, Yashinaka R, Oda M (1974) Weathering and its relation to mechanical properties of granite. In: Proc 3rd Int Congr Intyernational Society of Rock Mechanics, Denver 71–78
Persaud M, Pfiffner OA (2004) Active deformation in the eastern Swiss Alps: post-glacial faults, seismicity and surface uplift. Tectonophysics 385:59–84
Selby MJ (1993) Hillslope material and processes. Edition Oxford. Second edition 445
Storti F, Billi A, Salvini F (2003) Particle size distribution in natural carbonate fault rocks: insights for non-self-similar cataclasis. Earth Planet Sci Lett 206:173–186
Terzaghi K (1967) Soil mechanics in engineering practise. Wiley, New York, 729
Tric E, Lebourg T, Jomard H, Lecossec J (2010) Study of large-scale deformation induced by gravity on the La Clapière landslide (Saint-Etienne de Tinée, France) using numerical and geophysical approaches. J Appl Geophys 70:210–215
Zelasko JS (1966) An investigation of the influences of particles size, size gradation and particle shape on the shear strength and packing behaviour of quarziferous sand. Ph D. Thesis, North-western University, Evanston

T. Lebourg (✉) · H. Mickael · B. Thomas · Z. Swann · T. Emmanuel · V. Maurin
UMR 6526, Géoazur, CNRS-UNSA-IRD-UPMC,
250 rue A. Einstein, 06560, Valbonne, France
e-mail: lebourg@geoazur.unice.fr

J. Hervé
Institut of Radioprotection and Nuclear Safety (IRNS),
Fontenay-aux-Roses, France

E. B. Samyr
LRPC Nancy,
71 rue de la Grande Haie, 54510,
Tomblaine, France